

## Controls of the basal mass balance of floating ice shelves

D. E. Gwyther<sup>1,2</sup>, B. K. Galton-Fenzi<sup>2</sup> and J. L. Roberts<sup>3,2</sup>

<sup>1</sup>Institute for Marine and Antarctic Studies,  
 University of Tasmania, Private Bag 129, Hobart, Tasmania 7001, Australia

<sup>2</sup>Antarctic Climate & Ecosystems Cooperative Research Centre,  
 University of Tasmania, Private Bag 80, Hobart, Tasmania 7001, Australia

<sup>3</sup>Department of Sustainability, Environment, Water, Population and Communities,  
 Australian Antarctic Division, Hobart, Tasmania, Australia

### Abstract

Models of the circulation beneath ice shelves draw on knowledge gained from observations of the turbulent boundary layer beneath sea ice [1] to parameterise the thermodynamic interaction between ice-shelf and ocean [2]. These parameterisations are commonly transferred to the sub-ice-shelf boundary layer in regions of melting [3], but are limited by uncertainty in the value of the friction coefficient and representations of the heat flux into the ice shelf and are wholly unsuitable when the nature of the ice-ocean interface is different [4], as a result of frazil formation in the super cooled waters. This paper will present an overview of the commonly used parameterisations and highlight where uncertainties remain.

### Introduction

Ice shelves primarily originate as snow, accumulated on the ice sheet, which flows outwards to the ocean and form where the ice sheet detaches from the bedrock as it starts to float. In Antarctic oceans, ice shelves can vary in thickness from 100 m to over 2500 m (for example [5]), and southwards of the continental shelf break they cover 40% of the ocean [2]. An ocean filled cavity exists beneath ice shelves that is insulated from direct interaction with the atmosphere.

Since ice shelves are already floating, any change to their mass causes negligible sea level rise contribution [6]. However, as ice shelves act to buttress the ice sheet, which is grounded (and thus can contribute to sea level rise), the thermodynamic interaction of ice shelves and the ocean has important implications for sea level rise. For example, the west Antarctic ice sheet contains ice that if discharged into the ocean would lead to over 6 m of sea level rise [7].

It is thought that changes in basal melting of ice shelves, (driven by ocean circulation and temperatures) is the key factor in the thinning of several Antarctic glaciers [8]. Ice-ocean interaction processes are thus the dominant controlling mechanism of Antarctic mass loss. This paper reviews the present state of the understanding of the interaction between ice shelves and oceans, highlighting some key uncertainties. These parameterisations have their foundations in observations below sea ice [1] - a far more accessible environment - though they have been extended to ice shelf-ocean interaction processes (for example [2], [9] & [10]).

### Basal mass balance processes

The basal mass balance of ice shelves is controlled by gains from the input glacier; direct snow accumulation and basal freezing; and losses from basal melting and iceberg calving.

Ocean water that enters the cavity below ice shelves is usually above the *in situ* freezing temperature, due to the depression of

the freezing temperature with increasing pressure (and depth). This results in melting in the regions where water, warmer than freezing temperature, contacts the ice. The meltwater that is released is both colder and fresher and dilutes the seawater, to form water called Ice Shelf Water (ISW). Since ISW is more buoyant, it rises along the underside of the ice shelf as a buoyant plume [11]. As ISW rises, it can become cooler than the *in situ* freezing temperature and frazil can form in the water column. As the frazil grows it accretes upwards onto the ice shelf base as marine ice. Observations of marine ice indicate considerable thicknesses are possible (for example, 300 m [4]).

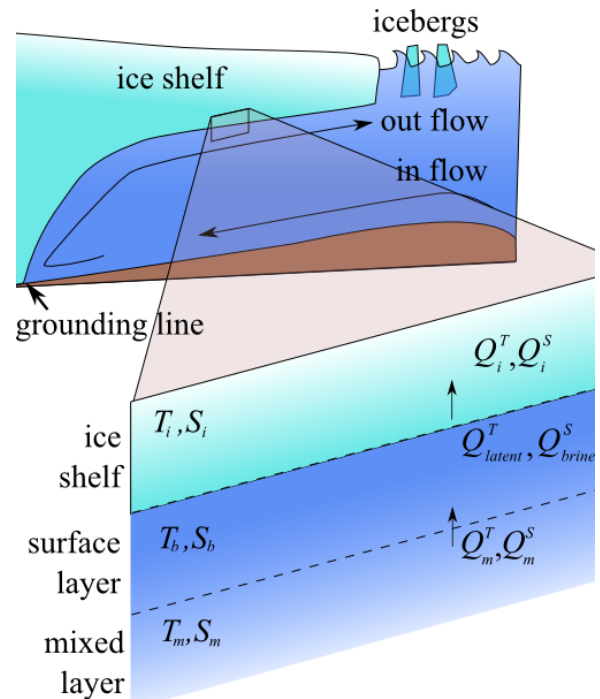


Figure 1: The ice-ocean interface at the base of an ice shelf is characterised by three regions; the ice, the surface layer, and the mixed layer, which describes far-field ocean conditions. The surface layer contains the interfacial sublayer.  $T$ ,  $S$ , and  $Q$  refer to temperature, salinity and flux, respectively. The subscripts  $i$ ,  $b$  and  $m$  refer to the ice shelf, the surface layer and the mixed layer, while *latent* and *brine* refer to processes of melting/freezing and dilution of the ocean.

The interaction between the ice shelf and the ocean occurs in a 'surface' layer immediately adjacent to the ice shelf that is  $\sim 1$  m thick and an outer mixed layer  $\sim 10$  m thick. Within the surface layer, direct interaction between the flow and the surface roughness occurs (figure 1). Heat and salt enter the surface

layer from the ocean below and turbulent mixing carries heat and salt across the surface layer to the interface. Oceanic transport of heat to the base can cause melting, which will alter the salt balance within the surface layer and the *in situ* freezing temperature. Basal freezing occurs when ocean temperatures are below the freezing point temperature in the surface layer. Frazil accretion is the dominant mechanism of basal ice accumulation which is not included in the parameterisation presented below and as such, the parameterisation is expected to be unsuitable for regions of marine ice formation. The ice shelf-ocean interaction processes are governed by the rates that heat and mass exchange between the ice and the ocean. These interactions are described below.

### Heat Balance

The equation that describes the heat conservation at the ice-ocean interface is  $Q_{latent}^T = Q_i^T - Q_m^T$  (figure 1). Where  $Q_i^T$  is the heat flux through the ice ( $\text{J m}^{-2} \text{s}^{-1}$ ) and  $Q_m^T$  ( $\text{J m}^{-2} \text{s}^{-1}$ ) is the heat flux from the mixed layer into the surface layer. The latent heat flux, that goes to melting the ice is  $Q_{latent}^T = \rho_i m L_f$  ( $\text{J m}^{-2} \text{s}^{-1}$ ), where  $\rho_i = 916 \text{ kg m}^{-3}$  is the density of ice and is a function of both pressure and temperature, but is treated as constant,  $L_f = 3.34 \times 10^5 \text{ J kg}^{-1}$  is the latent heat of fusion of ice and  $m$  is the vertical velocity ( $\text{m s}^{-1}$ ) of the base of the ice shelf (positive when melting).

The heat flux conducted into the ice is  $Q_i^T = \rho_i c_i \kappa_i \frac{\partial T_{ice}}{\partial z} \Big|_b$ . Where the specific heat capacity of ice  $c_i = 2007 \text{ J kg}^{-1} \text{ K}^{-1}$  and the thermal diffusivity of ice,  $\kappa_i = 1.14 \times 10^{-6} \text{ m}^2 \text{ s}^{-1}$  are well known. The main uncertainty is attributing the temperature gradient through the ice. In practice, this can prove very difficult for unknown flow properties of ice, and thus use in ocean models requires several simplifications relating to the movement or advection of ice, and vertical diffusion of heat through the ice. A range of assumptions can be used. These are the ice is a perfect insulator (no advection or diffusion), ice that conducts heat but is not moving, (no advection, vertical diffusion) or ice that conducts heat and is moving (vertical advection, vertical diffusion). The latter condition gives a non-linear temperature gradient, if ice is added to the surface at the rate it is melted (steady state assumption). A further parameterisation of the temperature gradient would be to assume time and space varying vertical advection, but this would lead to intense computational problems. In nature, ice tends to retain a ‘memory’ of the freeze and melt history (such as previous temperature) experienced by that ice column, and so the best solution would be a fully coupled ice sheet - ice shelf - ocean model.

The heat flux into the surface layer is  $Q_m^T = \rho_m c_m \kappa_m \frac{\partial T_m}{\partial z} \Big|_b$ , where  $\rho_m = 1025 \text{ kg m}^{-3}$  is the mixed layer density,  $c_m = 3974 \text{ J kg}^{-1} \text{ K}^{-1}$  is the mixed layer specific heat capacity and  $\kappa_m$  is the thermal diffusivity of the water. The temperature gradient across the mixed layer is approximated to be linearly proportional to  $Nu$  as  $\frac{\partial T_m}{\partial z} \Big|_b = Nu \frac{T_b - T_m}{h}$ , with the Nusselt number  $Nu$ , describing the ratio of total heat transfer to conduction alone,  $T_b$  is the surface layer temperature,  $T_m$  is the temperature of the mixed layer and layer thickness is  $h$ . A thermal exchange velocity,  $\gamma_T$  is defined by grouping  $Nu$ ,  $\kappa_m$  and  $h$ . This can be recognised as  $\gamma_T = \Gamma_T u_*$ , where  $\Gamma_T$  is a dimensionless turbulent transfer coefficient and  $u_*$  is the friction velocity.  $u_*$  is related to the velocity of the water in the mixed layer (relative to the ice),  $U$ , by a dimensionless drag coefficient,  $C_d$  as,  $u_*^2 = C_d U |U|$ . The sensitivity of the interaction to the choice of the drag coefficient is shown later. The heat flux into the surface layer is captured by  $Q_m^T = \rho_m c_m \Gamma_T u_* (T_b - T_m)$ .

The heat conservation equation is therefore,

$$\rho_i m L_f = \rho_i c_i \kappa_i \frac{\partial T_i}{\partial z} \Big|_b - \rho_m c_m u_* \Gamma_T \cdot (T_b - T_m). \quad (1)$$

### Salt Balance

Analogous to equation (1), the equation for the salt conservation is  $Q_{brine}^S = Q_i^S - Q_m^S$  (figure 1). Here, the salt flux through the interface is  $Q_{brine}^S = \rho_i m (S_i - S_b)$ , where  $S_i$  and  $S_b$  are the salinities of the ice and surface layer respectively,  $Q_i^S$  ( $\text{psu m}^{-1} \text{ s}^{-1}$ ) is the diffusive flux of salt into the ice and  $Q_m^S$  ( $\text{psu m}^{-1} \text{ s}^{-1}$ ) is the flux of salt into the surface layer.  $S_i$  is assumed to be zero, which is very close for continental ice. However marine ice can contain brine inclusions, with salinities  $\sim 0.1$  psu [4]. The diffusive flux of salt in the ice,  $Q_i^S = 0$ , as salt cannot diffuse through the solid ice matrix. By analogy to the heat flux through the mixed layer, the salt flux through the surface layer is  $Q_m^S = -\rho_m u_* \Gamma_S \cdot (S_b - S_m)$ , where  $S_m$  is the mixed layer salinity. The turbulent transfer coefficient for salt,  $\Gamma_S$ , is a dimensionless mass analogy of the thermal Stanton number, which describes the diffusion rate of salt. For the surface layer, close to the ice shelf-ocean interface,  $\Gamma_S$  is approximately two orders of magnitude smaller than  $\Gamma_T$ . It is only in the fully turbulent area of the surface layer (where eddy suppression from the interface is negligible) that thermal and saline diffusivities (and hence, the corresponding transfer coefficients) can be assumed to be equal [2]. The salt balance at the surface layer is

$$\rho_i m (S_b - S_i) = -\rho_m u_* \Gamma_S \cdot (S_b - S_m). \quad (2)$$

### Freezing Temperature Dependence

$T_b$  is at the local freezing temperature and is a linear function of pressure and a weakly non-linear function of salinity [12]. We use the linearised relationship to simplify solving for the melt rate. The linearised version of this relationship is

$$T_b = \lambda_1 S_b + \lambda_2 + \lambda_3 P_b, \quad (3)$$

where  $\lambda_1 = -5.73 \times 10^{-2} \text{ }^\circ\text{C}$  is the liquidus slope,  $\lambda_2 = 9.39 \times 10^{-2} \text{ }^\circ\text{C}$  is the liquidus intercept and  $\lambda_3 = -7.53 \times 10^{-8}$  is the liquidus pressure coefficient, and are chosen so to maximise the linearisation fit.  $S_b$  and  $P_b$  are the surface layer salinity and pressure. The deviation of the linearised fit from the full equation for freezing temperature is shown later. All present ice shelf-ocean models use equations (1), (2) and (3) and rearrange to solve for  $m$ ,  $S_b$ ,  $T_b$ .

### Key uncertainties

The physical constants or properties of ice and water (such as  $\rho_{i,m}$ ,  $c_{i,m}$ ,  $\kappa_{i,m}$ ) are well known. However, the turbulent transfer coefficients,  $\Gamma_{T,S}$  and the coefficient of drag are empirical descriptions of the turbulence parameters, based on sparse measurements of potentially dissimilar systems [13]. Authors have argued that these laboratory-derived expressions should hold for realistic scenarios, but doubt remains whether they will be representative in the case of an ice shelf, with strong buoyant plumes and uncertain basal roughness (see [3, 2]). For example, it is debated whether surface roughness has a bearing on the transfer coefficient, as there is a disagreement between laboratory results and observations beneath sea ice [1].

In ocean models,  $C_d$  is typically assumed constant, even though it is a function of the characteristic roughness scale of the surface,  $z_0$  and the current profile,

$$C_d = \left( \frac{\kappa}{\ln(z/z_0)} \right)^2 \quad (4)$$

where  $\kappa = 0.41$  is the von Kàrmàn constant. The value of  $C_d$  is typically calculated at a reference distance of 1 m from the interface ( $z = 1$  m), and thus can be combined into the parameterisation of  $u_*$ . The parameterisation of  $C_d$  was originally developed for atmospheric boundary layers [14], and was initially applied to turbulence studies under sea ice, but is complicated in this application by the different basal conditions [4, 3]. The roughness scales that exist sub-ice shelves are wide, ranging from  $1 \times 10^{-3}$  m, to much larger features such as crevasses and rifting spanning  $\sim 100$  m. The geographical constraints makes studying the physical environment to choose parameters relevant to equation (4) exceptionally difficult and as a result, will remain elusive until extensive field measurements can be made.

Both the buoyancy driven currents and tidal currents are important to the friction velocity,  $u_*$ . Buoyant plumes are adequately simulated within models, but the limited spatial and temporal distribution of ocean current observations made by moorings beneath ice shelves, restricts the use of observations to constrain parameterisations of currents beneath ice shelves. Many models do not include realistic tidal currents and thus friction velocities in their parameterisations are underestimated. Recent studies have assumed constant ocean currents,  $U$ , under the ice shelf [15], however it has been shown that this will mispredict spatial distribution of melt and freeze regions [16]. It is therefore important to include realistic simulations of sub-ice currents by including tides.

The choice of description of  $T_b$ , given in equation (3) is the linearised version of the true, non-linear relationship. Since  $T_b$  is one of the three equations needed to be solved simultaneously, it is computationally efficient to use the linearised equation. Linearisation of  $T_b$  introduces an error, as shown in figure 2, which becomes important with depth.

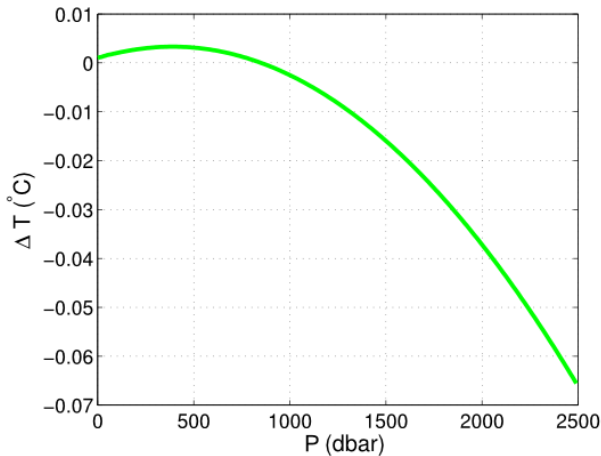


Figure 2: The difference between linearised and non-linearised TEOS-10 [12] freezing temperature as a function of depth is shown (with salinity constant at 34.4 psu).

To demonstrate the effect of uncertainty in the parameterisation variables on the basal melt rates, we report several sensitivity studies. The first study investigates the choice of  $C_d$ , for different thermal forcing values,  $T^* = T_m - T_b$  (see figure 3). With a small thermal forcing, the choice of  $C_d$  is less important. However, at high  $T^*$ , melt rate is dependent on  $C_d$ . Considering that the regions that demonstrate rapid thinning, such as Pine Island Glacier [8], also exhibit strong in-flow of water well above the *in situ* freezing temperature (i.e. large  $T^*$ ) then it is expected that the choice of  $C_d$  is important.

The choice of parameterisation of the temperature profile

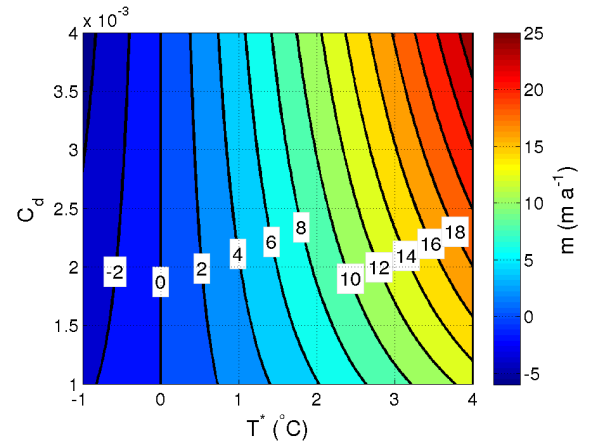


Figure 3: The melt rate as determined by the above parameterisation, for a range of  $T^*$  and  $C_d$ . Contours are labeled for melt rate.

through the ice shelf is also important for the melt rate, which is constrained by the annual average temperature at the surface ( $\sim -20^\circ\text{C}$ ) and at the base by the freezing temperature. Observations and modelling show the temperature profile between the surface and base is dependent on melt rate [17]. Strong melting causes rapid temperature drop to cold internal temperatures over a short length, as ice is being removed before the temperature of the interior can equilibrate. For freezing regions the curve is reversed, with temperatures close to  $T_b$  for most of the profile, before it rapidly asymptotes to the surface temperature. To correctly parameterise heat flux into the ice shelf, the gradient of temperature evaluated at the base of the ice shelf,

$$\left. \frac{\partial T_i}{\partial z} \right|_b \quad (5)$$

must be determined. We examine 4 cases; A, assume a linear temperature profile, varying from surface to freezing temperature over very small  $\partial z$ ; B, assume a linear temperature profile, varying from the surface temperature to the freezing temperature, over large  $\partial z$ . Both of these are linear profiles; C, a more realistic non-linear profile is achieved by assuming constant vertical advection and vertical diffusion [2]. The resulting parameterisation is valid under high melt rates greater than  $\sim 0.2$  m  $\text{s}^{-1}$  and for thick ( $\geq 1000$  m) ice shelves; and D, assuming insulating ice, i.e. the ice is at basal freezing temperature.

The effect of the 4 parameterisations of equation (5) on the melt rate is shown in figure 4. High  $T^*$  leads to high melt rates with all parameterisation of ice temperature profile. At high thermal forcing, A, B and D all over-estimate melt rate, because they do not capture the ability of heat to diffuse quickly upwards through the shelf. Only C, which includes the vertical velocity of ice, correctly captures the magnitude of the gradient for high melt rates. When  $\partial z$  is small, A, switches to a freezing regime at very low but non-zero thermal forcing. This switch to freezing captures the effect of heat conduction upwards into the ice exceeding the supply of heat into the surface layer from the mixed layer. B and D both have shallow temperature gradients, and thus energy is not removed quickly, and melt rates go to zero with the thermal forcing. The profile with advection and diffusion, C, also does not describe the melt-to-freeze flip accurately as approximations were made which do not hold at low melt rates.

Problems exist in all parameterisations of the ice temperature profile. The most advanced description, with constant vertical advection and diffusion, which describes high melting scenarios well, includes approximations which are not applicable at low

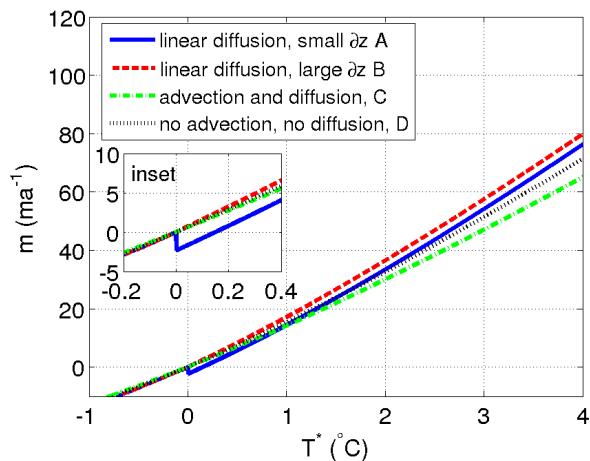


Figure 4: Melt rate ( $\text{m a}^{-1}$ ) is shown as a function of the thermal forcing, for different ice temperature profiles. These profiles are linear diffusion (small  $\partial z$ , case A, large  $\partial z$  ice case B), advection and diffusion, case C, and the no advection and no diffusion case D.

melt rates or thin ice shelves. Similarly, the other cases here do not describe high melt rate scenarios well. An argument could be made to use the low  $\partial z$  ice, linear temperature profile, which describes low thermal forcing scenarios well, as it is thought that while several ice shelves show high melting at great depth, there are large areas of thinner ice at low thermal forcing values - an effect not captured by the most advanced parameterisation.

## Conclusions

The parameterisation of the thermodynamic interaction between the ocean and ice shelves is fundamental to calculating accurate melt rates in ocean models. This is particularly important for calculating contributions towards global sea level rise. We have presented an overview of the current and 'best' parameterisations of this interaction, and highlighted areas where uncertainties exist. These uncertainties exist in the parameterisation itself, in the choice of parameters, as well as problems relating to the geographical constraints placed on making observations in a sub-ice shelf environment. This has highlighted the need for further investigation of the parameterisation and in particular, development of integrated ocean-ice shelf-ice sheet models.

## Acknowledgements

This work was supported by the Australian Government's Cooperative Research Centre Programme through the Antarctic Climate & Ecosystems Cooperative Research Centre. David Gwyther is supported by the CSIRO and UTAS through the QMS PhD program. Thanks to John Hunter for reading and improving an early draft.

## References

[1] McPhee, M. G., *Air-Ocean Interaction: Turbulent Ocean Boundary Layer Exchange Processes*, Springer, 2008

[2] Holland, D. M., & Jenkins, A.. Modeling Thermodynamic Ice-Ocean Interactions at the Base of an Ice Shelf. *Journal of Physical Oceanography*, 29(8), 1999, 1787-1800.

[3] Jenkins, A., Nicholls, K. W., & Corr, H. F. J. Observation and Parameterization of Ablation at the Base of Ronne

Ice Shelf, Antarctica. *Journal of Physical Oceanography*, 40(10), 2010, 2298-2312.

[4] Craven, M., Allison, I., Fricker, H. A., & Warner, R Properties of a marine ice layer under the Amery Ice Shelf, East Antarctica. *Journal of Glaciology*, 55(192), 2009, 717-728.

[5] Galton-Fenzi, B. K., Maraldi, C., Coleman, R., & Hunter, J. The cavity under the Amery Ice Shelf, East Antarctica. *Journal of Glaciology*, 54(188), 2008, 881-887.

[6] Noerdlinger, P. D., & Brower, K. R. The melting of floating ice raises the ocean level. *Geophysical Journal International*, 170(1), 2007, 145-150.

[7] Church, J. A. et al. (Eds.), *Climate Change 2001: The Scientific Basis: Contribution of Working Group I to the Third Assessment Report of the Intergovernmental Panel on Climate Change* (pp. 639-694). 2001, Cambridge University Press (Cambridge, New York).

[8] Pritchard, H. D., Arthern, R. J., Vaughan, D. G., & Edwards, L. A. Extensive dynamic thinning on the margins of the Greenland and Antarctic ice sheets. *Nature*, 461(7266), 2009, 971-5.

[9] Dinniman, M. S., Klinck, J. M., & Hofmann, E. E. Sensitivity of Circumpolar Deep Water transport and Ice Shelf Basal Melt along the West Antarctic Peninsula to Changes in the Winds. *Journal of Climate*, 5, 2012, 4799-4816.

[10] Galton-Fenzi, B. K., J. R. Hunter, R. Coleman, S. J. Marsland and R. C. Warner. 2012. Numerical modelling of Melt/Freeze beneath the Amery Ice Shelf, East Antarctica. *Journal of Geophysical Research - Oceans* (accepted).

[11] Lewis, E. L., & Perkin, R. G. Ice Pumps and Their Rates. *Journal of Geophysical Research*, 91(C10), 1986, 11756-11762.

[12] IOC, SCOR and IAPSO, *The international thermodynamic equation of seawater - 2010: Calculation and use of thermodynamic properties*. Intergovernmental Oceanographic Commission, Manuals and Guides No. 56, UNESCO (English), 196 pp, 2010

[13] Yaglom, A. M. and Kader, B. A. Heat and mass transfer between a rough wall and turbulent fluid flow at high Reynolds and Péclet numbers. *Journal of Fluid Mechanics*, 62(03), 1974, 601-623.

[14] Paulson, C. The mathematical representation of wind speed and temperature profiles in the unstable atmospheric surface layer. *Journal of Applied Meteorology*, 1970, 857-861.

[15] Holland, P. R., Jenkins, A., & Holland, D. M. The Response of Ice Shelf Basal Melting to Variations in Ocean Temperature. *Journal of Climate*, 21(11), 2008, 2558-2572.

[16] Mueller, R. D., Padman, L., Dinniman, M. S., Erofeeva, S. Y., Fricker, H. A., & King, M. A. Impact of tide-topography interactions on basal melting of Larsen C Ice Shelf, Antarctica. *Journal of Geophysical Research*, 117(C5), 2012, 1-20.

[17] Humbert, A. The temperature regime of Fimbulisen, Antarctica. *Annals of Glaciology*, 51(55), 2010, 56-64.